The possible use of combined electrical impedance and ultrasound velocity measurements for the non-invasive measurement of temperature during mild hyperthermia

2013 Physiol. Meas. 34 1103

(http://iopscience.iop.org/0967-3334/34/9/1103)

OPEN ACCESS
IOP PUBLISHING PHYSIOLOGICAL MEASUREMENT
Physiol. Meas. **34** (2013) 1103–1122 doi:10.1088/0967-3334/34/9/1103

The possible use of combined electrical impedance and ultrasound velocity measurements for the non-invasive measurement of temperature during mild hyperthermia

Naimul Islam[1,2], **Rebecca Hale**[1], **Matthew Taylor**[1] **and Adrian Wilson**[1,3]

[1] Department of Physics, University of Warwick, Gibbet Hill Road, Coventry, CV4 7AL, UK
[2] Department of Physics, University of Dhaka, Dhaka-1000, Bangladesh
[3] Department of Clinical Physics and Bioengineering, University Hospital, Coventry CV2 2DX, UK

E-mail: adrian.wilson@warwick.ac.uk

Received 14 May 2013, accepted for publication 23 July 2013
Published 23 August 2013
Online at stacks.iop.org/PM/34/1103

Abstract

This paper explores the possibility of using combined measurements of electrical impedance and changes in ultrasound time of flight for determining deep body temperature during mild hyperthermia. Simultaneous electrical impedance spectra (1 kHz–1024 kHz) and ultrasound time-of-flight measurements were made on layered sheep liver and fat tissue samples as the temperature was increased from 30–50 °C. The change in propagation velocity for 100% fat and 100% liver samples was found to vary linearly with temperature and the temperature coefficient of the time-of-flight was shown to vary linearly with the % fat in the sample (0.009% $^{\circ}C^{-1}\%^{-1}$). Tetrapolar impedance measurements normalized to 8 kHz were shown to have a small sensitivity to temperature for both liver (0.001% $^{\circ}C^{-1} \leqslant 45$ °C) and fat (0.002% $^{\circ}C^{-1} \leqslant 512$ kHz) and the best linear correlation between the normalized impedance and the % fat in the sample was found at 256 kHz (gradient $0.026\%^{-1}$, $r^2 = 0.65$). A bootstrap analysis on 15 layered tissue samples evaluated using the normalized impedance at 256 kHz to determine the % fat in the sample and the temperature coefficient of the time of flight to determine the temperature. The results showed differences (including some large differences) between the predicted and measured temperatures and an error evaluation identified the possible origins of these.

Keywords: electrical impedance, ultrasound, temperature

1. Introduction

Mild hyperthermia, in which a tumour but not the surrounding tissue is selectively heated to between 41 and 43 °C, has been shown to give improvements in tumour control and five year survival rate when used in conjunction with radiotherapy or chemotherapy (Triantopoulou *et al* 2013, Sauer *et al* 2012, ter Haar 1999). Currently the technique is only applicable to surface tumours and tumours that can be accessed through body cavities due to problems of producing controlled localized heating deep within the body (Lagendijk 2000, van Rhoon and Wust 2005). We have recently reported the design principles for a phased array ultrasound transducer capable of creating localized heating of solid tumours deep within the body (Aitkenhead *et al* 2008, 2009) but the problems of non-invasive temperature measurement to achieve control remain unresolved. A variety of temperature dependent physical properties have been investigated to address this problem including ultrasound propagation velocity (Miller *et al* 2002, 2004, Seip and Ebbini 1995), ultrasound back scattered energy (Staube and Arthur 1994, Arthur *et al* 2003), electrical impedance imaging (Conway *et al* 1985, Paulson and Jiang 1997, Ferraioli *et al* 2009) and relaxation times in magnetic resonance imaging (MRI) (Rieke and Pauly 2008). Mild hyperthermia treatments can last up to an hour and therefore temperature measurement methods based on electrical impedance or ultrasound are more appropriate than techniques based on MRI. Work on ultrasound backscattered energy was based on synthetic scatterers introduced into the tissue (Arthur *et al* 2003) and thus is not truly non-invasive and, in addition, the thermal properties of the tissue containing the scatterers is unknown. Therefore a technique based on ultrasound propagation velocity or electrical impedance, in particular a technique based on ultrasound propagation velocity using the same ultrasound transducer to create mild hyperthermia and to measure temperature, would be particularly attractive.

The published data on ultrasound propagation velocity show aqueous cellular tissues (e.g. liver) to peak at about 50 °C having a positive propagation velocity temperature coefficient below this temperature and a negative propagation velocity temperature coefficient above it, whilst fat has a negative propagation velocity temperature coefficient for all temperatures (Bamber 1998). Using the analyses from Chambre (1959) and Apfel (1983) it can be shown that the total propagation velocity c_T for a mixture of N chemically non-reacting materials is given by:

$$\frac{1}{c_T} = \sum_{i=1}^{N} \frac{f_i}{c_i} \tag{1}$$

where f_i and c_i are the fractional volume and propagation velocity of the ith component of the mixture respectively. The propagation velocity of pure water as a function of temperature was measured at atmospheric pressure by Del Grosso and Mader (1972) and found to rise up to 75 °C and then fall thereafter. Using these data, a fifth order polynomial was used to describe the propagation velocity versus temperature profile (Del Grosso and Mader 1972). This change in the propagation velocity with temperature is a result of the compressibility of the water molecule (Kell 1975). In addition to ionic intra- and extra-cellular fluids, which have the propagation velocity characteristics of water, aqueous cellular tissues contain condensed matter (mostly lipids, elastin and collagen) which have a negative change in propagation velocity with temperature. The combined propagation velocity of these components gives liver (and other aqueous tissues) a peak in the measured propagation velocity at around 50 °C (Bamber 1998), a finding that can be predicted using equation (1) (Miller *et al* 2002). One application of the previous work on ultrasound propagation velocity was aimed at identifying the target volume for high intensity focused ultrasound (HIFU) treatments

(Miller *et al* 2002, 2004). In order to do this it was proposed to operate the HIFU transducer at pre-ablative intensities so that the temperature rise was less than 50 °C, otherwise the changes in propagation velocity would be non-unique. Since the objective of this work was visualization of the volume to be heated rather than temperature measurement, the effect of any nonlinearity in the propagation velocity versus temperature characteristic up to 50 °C could be ignored.

The physical principle behind using electrical impedance measurements for determining temperatures is that the conductivity of physiological saline changes by about 2% $°C^{-1}$ and was one of the early applications proposed for electrical impedance tomography (Conway *et al* 1985). Work on the electrical impedance of living tissue showed that the observed impedance changes were not simply due to changes in conductivity of the intra- and extra-cellular fluids but also due to intra- and extra-cellular fluid volume changes and membrane conductance changes (Esrick and McRae 1994). Gersing (1999) suggested that extra-cellular volume changes resulting from vasodilatation was the primary effect and that this occurred concurrently with heating in normal tissue but was delayed in cancerous tissue. Paulson and Jiang (1997) proposed improvements in an electrical impedance image reconstruction technique which, in a simulation study, reduced the errors in temperature prediction from the order of 10 °C reported by many workers (e.g. Moskowitz *et al* 1994) to 2 °C. However, this accuracy is unlikely to be achieved in clinical practice using electrical impedance measurement from patients and is above the 1 °C accuracy normally cited for the clinical application of mild hyperthermia. All the work on electrical impedance measurements to measure temperature during hyperthermia has used a tetrapolar impedance measurement technique. Whilst tetrapolar measurements eliminate the effect of the electrode impedances, which can be very much larger than those of the tissue, the spatial sensitivity is complex and contains maxima beneath the edges of the electrodes and regions of negative sensitivity between the drive and receive electrodes (Brown *et al* 2000a, Islam *et al* 2010). This complex spatial sensitivity distribution gives an uncertainty in the position of any impedance changes related to temperature and is likely to be the source of the poor correlations reported between changes in electrical impedance and temperature.

Both ultrasound propagation velocity and electrical impedance are potential techniques to measure the temperature during mild hyperthermia for deep body solid tumours. The previous work in this area has demonstrated that neither method has the capability to non-invasively measure temperature to the accuracy required for clinical mild hyperthermia. In both cases, with the exception of the electrical impedance study by Gersing (1999), the work has been carried out using imaging devices and the effect of the image processing algorithms on the results reported is unknown although this is likely to be greater for electrical impedance than ultrasound because of the need for image reconstruction and the complex spatial sensitivity in the former. Therefore in this paper we report a first experimental investigation into the potential of simultaneous measurements of ultrasound propagation velocity and electrical impedance as an approach to non-invasively measuring temperature in deep body mild hyperthermia.

2. Materials and methods

In this work we used a Perspex test cell that allowed simultaneous tissue impedance and ultrasound propagation velocity measurements on tissue samples (figure 1). The temperature of the tissue sample in the test cell was controlled in the range 30–50 °C by placing the cell in a thermostatically controlled water bath.

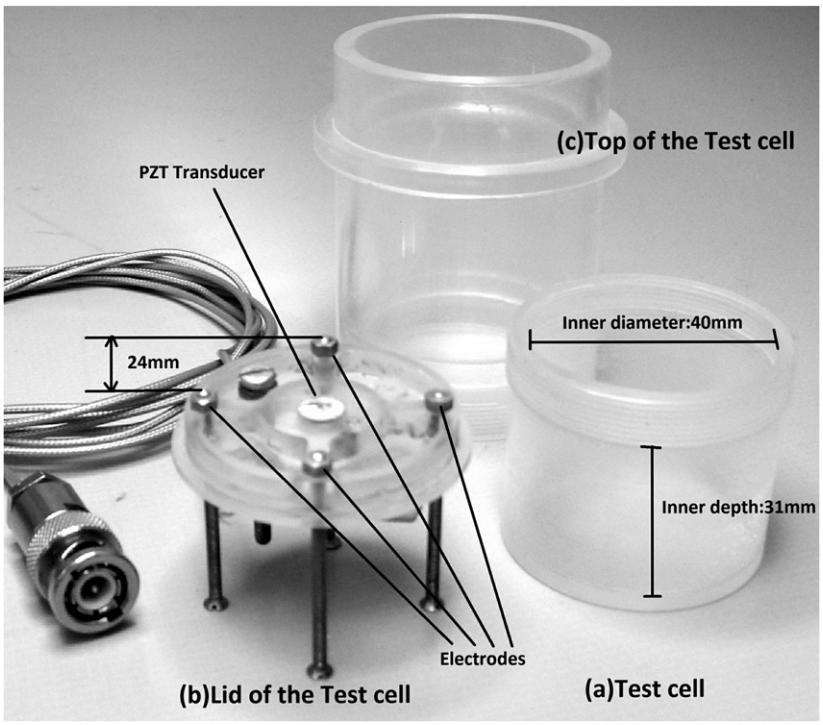

Figure 1. An annotated photograph of the Perspex test cell showing the positions of the electrodes and PZT element. The 'inner depth' of the cell is the distance between the front face of the PZT element and the inner surface of the base of the cell.

2.1. Test cell

The part of the test cell holding the sample is cylindrical with a diameter of 40 mm and a depth of 36 mm. A wall thickness of 2 mm was used as a compromise between robustness and thermal resistance. The top of the test cell contained four 2.5 mm diameter stainless steel/brass electrodes for electrical impedance measurements and a 7 mm diameter circular 1 MHz lead zirconate titanate (PZT) element (PZT-8, Sparkler Ceramics Ltd, India) for ultrasound propagation velocity measurement. The four electrodes for electrical impedance measurement were equi-spaced at a radius of 17 mm from the centre forming the corners of a square giving an electrode spacing of 24 mm. We have previously shown that for four electrodes arranged in a square there is a peak in the average sensitivity of a plane at a depth of 1/3 of the electrode separation (Brown *et al* 2001a, Islam *et al* 2010)—a depth of 8 mm in the test cell. If it is assumed that the circular PZT element behaves as a piston, then the axial intensity profile in the direction of propagation has the form of a Bessel function of the first type with the last axial maxima at a^2/λ where a is the radius of the transducer and λ is the wavelength in the media. The value of λ for 1 MHz ultrasound in soft tissue is approximately 1.5 mm. A PZT transducer of 7 mm in diameter was selected to position the last axial maxima at a depth of 8 mm. Thus the maxima in the sensitivity of the electrical impedance and ultrasound intensity are collocated in the sample chamber. Tissue samples in the sample chamber were heated by placing the test cell in a water bath created from a 1000 ml beaker placed on top of a thermostatically controlled hotplate (Fisher Scientific 11–302–508 HP). Throughout the measurements the tissue temperature was measured with a thermocouple

positioned in the tissue sample at approximately half the depth of the test cell and at a radius of 15 mm from its centre line. This thermocouple was connected to a calibrated electronic thermometer (Digitron 2038T). Electrical impedance and ultrasound propagation velocity measurements were under computer control where the computer could trigger simultaneous measurements.

2.2. Ultrasound measurement instrumentation

One of the design principles for our proposed ultrasound transducer to create deep body mild hyperthermia (Aitkenhead *et al* 2008) was that the PZT elements were air backed allowing them to ring undamped following the application of a drive pulse to avoid loss of energy due to absorption in the backing layer (Persson and Hertz 1985). Our aim was to use the same arrangement for mounting the PZT element for this study as was used in that transducer. However, for ultrasound propagation velocity measurements where the same element is to be used for transmission and echo detection, this results in unwanted ringing of the transducer at 1 MHz. To minimize the effect of this, the transducer was driven with a 1 μs pulse where the first minima in the frequency spectra was at 1 MHz generating a single isolated 1 μs pulse from the PZT element. Following excitation, the voltage from the PZT element was amplified and digitized at 100 MHz using the first channel of a two channel high speed USB digitizer (National Instruments, USB-5133). All data processing was performed in Matlab with a specially written C code routine used to transfer data from the data acquisition device to Matlab for processing. Data acquisition was triggered from the start of the transmitted pulse and twenty consecutive 100 μs data sets were averaged to improve the signal-to-noise ratio. Experimentally it was found that the transducer also generated sub-harmonic ringing at about 200 kHz on both transmission and detection. Therefore, following data acquisition and averaging an equi-ripple FIR band pass filter (length 284, passband 750 kHz–1.25 MHz) was used which provided greater than 40 dB attenuation of the 200 kHz component. The time of flight (ToF) between the transducer and the base of the test cell was determined by visually inspecting the 1 MHz reflected signal (figure 2).

2.3. Electrical impedance measurement instrumentation

Tetrapolar electrical impedance measurements were made using the same technique as that used in the Sheffield Mk3.5 electrical impedance temperature system (Wilson *et al* 2001). Current injection was achieved using a differential Howland current source circuit. Electrical impedance was measured simultaneously at 11 octave separated frequencies in the range 1–1024 kHz. The drive signal consisted of repeated 1 ms epochs of 11 summed sine waves such that repeated epochs provided a continuous sine wave at each frequency. Each frequency had a peak-to-peak amplitude of 200 μA giving a maximum drive current of 1.2 mA peak-to-peak. The voltage from the receive electrodes was amplified by a differential amplifier and then digitized using the second channel of the National Instruments high speed digitizer sampling at 10 MHz. As before (section 2.2) transfer of data from the digitizer to Matlab for processing was controlled by a C-code routine and all data processing was performed in Matlab. Twenty epochs of measured data were summed to improve the signal-to-noise ratio. A fast Fourier transform was performed on the averaged voltage data to determine the amplitude and phase spectrum for each of the drive frequencies and the former then scaled to determine the real part of the transfer impedance in ohms.

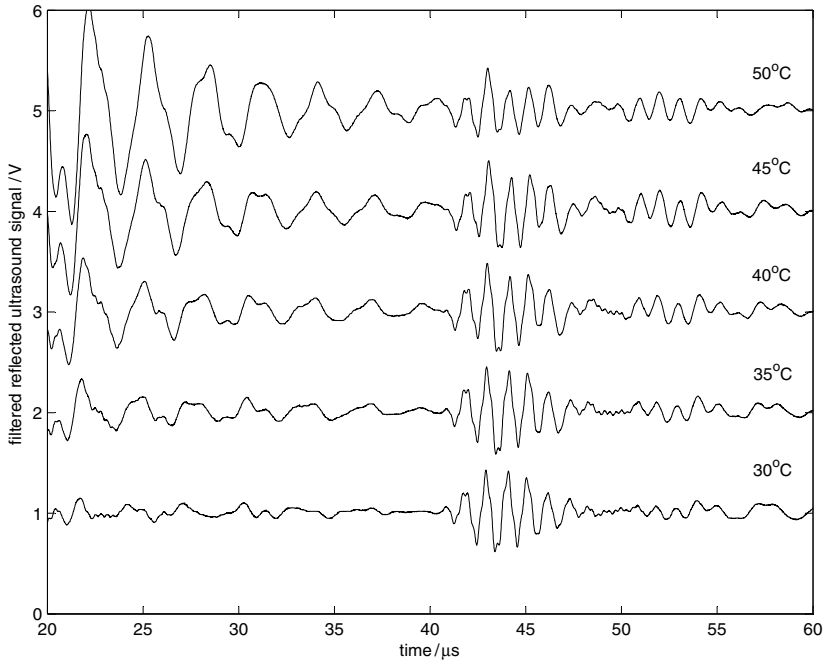

Figure 2. The reflected ultrasound signal in liver at 5 °C intervals between 30 °C and 50 °C showing the reflected pulse from the base of the chamber at approximately 42 μs. The signal for each temperature has been offset by 1 V.

2.4. Measurements

In this paper we report three sets of measurements: measurements on liver samples, measurements on fat samples and measurements on layered liver and fat samples. In all three cases, the tissue was obtained as fresh (never frozen) samples from sheep through retail butchers. For the single tissue measurements, 40 mm diameter samples were cut from the tissue and placed in the sample chamber in the form of layers. The typical layer thickness was 6 mm. For the layered tissue samples the numbers of layers of fat and liver were altered to simulate liver tissue containing different proportions of fat. Samples of liver were taken from tissue where there was no visible fat content. The density of the liver and fat used in these experiments was established by measuring the volume (using water displacement) and mass for samples taken from the bulk tissue from which the measurement samples were taken. The percentage of fat (expressed as a percentage by volume) in the final sample was then determined by weighing the fat and liver components of the sample after the measurement. For the single tissue measurements the propagation velocity was calculated from the ToF measured as the time to the first peak in the reflected signal from the base of the test cell and the distance between the PZT element and the base of the test cell. As noted by Bamber (1998), the ToF method for determining the propagation velocity is dependent on being able to reproducibly detect the time of arrival of the reflected signal. With the layered tissue samples, there were multiple tissue interfaces increasing the number of reflections resulting in a more complex reflected signal and reducing its amplitude. These made the first peak more difficult to detect and therefore the percentage change in ToF from a measurement at 30 °C was analysed based on the first large peak after 40 μs for the layered tissue experiments. The

electrical impedance spectra for the 100% fat and 100% liver samples were interpreted in terms of the spectrum expected based on a Cole–Cole model (Cole and Cole 1941) of how tissue structure affects impedance. It should be noted that the nature of the layered liver and fat sample meant that the percentage of fat in the different samples could not be accurately reproduced and therefore the reproducibility is based on the number of fat and liver layers in each sample and the relationship between the sample composition and the magnitude of the electrical impedance investigated using a line of best fit determined by the least squares method and the Pearson r correlation coefficient. Throughout the work the confidence interval for the slopes of the lines of best fit were calculated using the method of Liengme (2002) based on the t-statistic.

3. Results

3.1. Ultrasound propagation velocity results

The propagation velocities for six samples of liver and six samples of fat measured at 5 °C intervals between 30 and 50 °C are given in figures 3(a) and (b) respectively. From these figures it can be seen that there is a large variation in the absolute value of propagation velocity between samples for both tissue types (range is approximately 50 ms^{-1} for both at 35 °C) but that the changes in velocity with temperature for individual samples follow a similar trajectory. The focus of this work was non-invasively determining the temperature of a volume of tissue that is to be heated. Since the body temperature is closely controlled at 37 °C, determining the change in temperature from a pre-heated state is an acceptable approach. To investigate the feasibility of this approach the data were analysed by looking at the change in propagation velocity with temperature starting from the propagation velocity at 30 °C. The results for this analysis on the data shown in figures 3(a) and (b) are given in figures 4(a) and (b) respectively. Individual samples of the same tissue type are identified by the same symbols in figures 3 and 4.

In looking at the data in figures 3(a) and 4(a), it should be noted that the propagation velocities for the liver sample starting at approximately 1475 ms^{-1} (the sample with the star symbol in figure 3(a)) are always less than the other samples but it is not the one with the lowest rate of change of propagation velocity with temperature as shown in figure 4(a). Within the temperature range 30–50 °C the individual liver samples showed an approximately linear rise in the propagation velocity with temperature but a large difference in the slopes between samples. Taken together these data gave a line of best fit with a slope of 0.93 $ms^{-1}\,°C^{-1}$ but with a relatively low value of r^2 of 0.62. For the fat there was a decrease in propagation velocity with temperature of -4.7 $ms^{-1}\,°C^{-1}$ ($r^2 = 0.91$). In this work, propagation velocity has been measured at specific temperatures whereas in mild hyperthermia the propagation velocity would be measured and the lines of best fit in figures 4(a) and (b) used to determine the temperature in liver and fat respectively. The technique based on the t-statistic used to establish the 95% confidence interval for the slope of the line of best fit can be extended to determine the measurement error from using the propagation velocity to measure temperature (Liengme 2002). As with any measurement the confidence interval is dependent on the number of measurements made. Assuming ten measurements, the errors in predicting temperature from the lines of best fit in liver and fat are ± 4.3 °C and ± 1.7 °C respectively at 40 °C.

As noted in the methods section, multiple reflections in the layered tissue samples reduced the amplitude of the reflected signal making the start of the reflection from the base of the test cell more difficult to detect and therefore the ToF is reported for these experiments rather than propagation velocity. The change in the propagation velocity for liver and fat with temperature

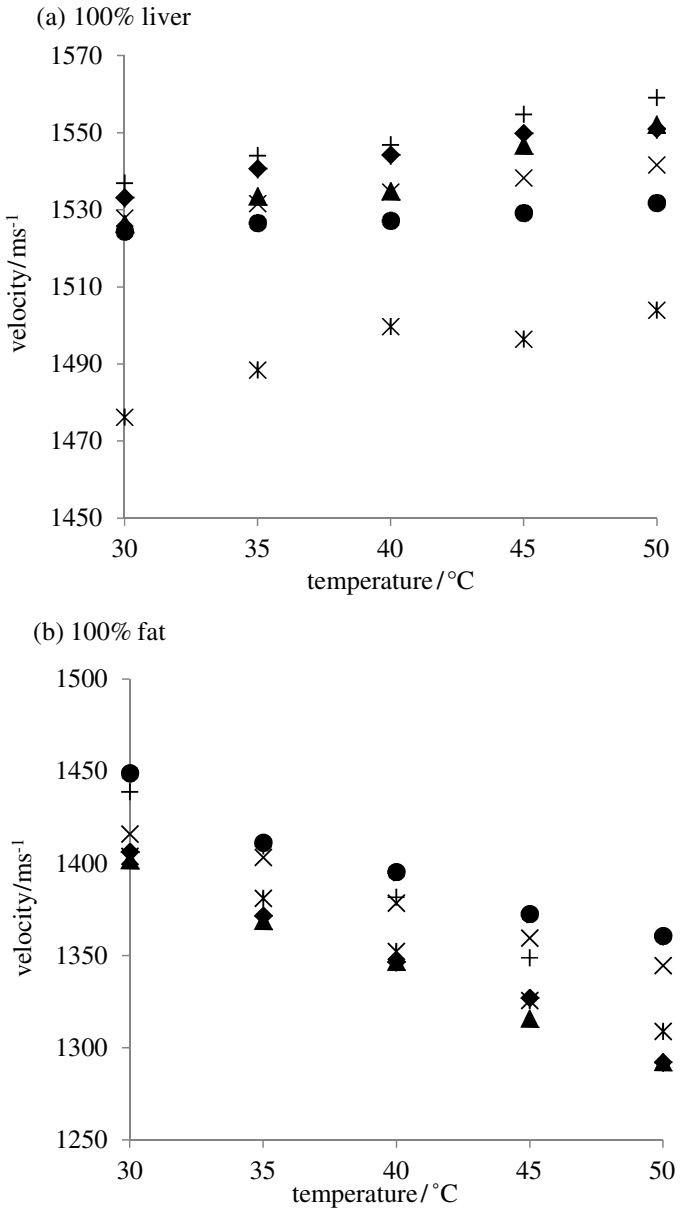

Figure 3. The propagation velocity of (a) 100% liver and (b) 100% fat with temperature. Individual samples of each tissue type are identified by symbols.

(figure 4) when combined with equation (1) predict straight line relationships between the change in ToF with temperature for mixtures of fat and liver where the gradient of the line increases as the fraction of fat in the sample increases. The results from measurements on 15 layered samples using the same measurement protocol as that used for the fat and liver confirm this prediction and give lines of best fit with gradients between $-0.06\%\ ^{\circ}\mathrm{C}^{-1}$ ($r^2 = 0.99$) for a sample with 0% fat to $0.7\%\ ^{\circ}\mathrm{C}^{-1}$ ($r^2 = 0.99$) for a sample with 100% fat. These data also allow investigation of how the temperature coefficient of the ToF (the percentage change in

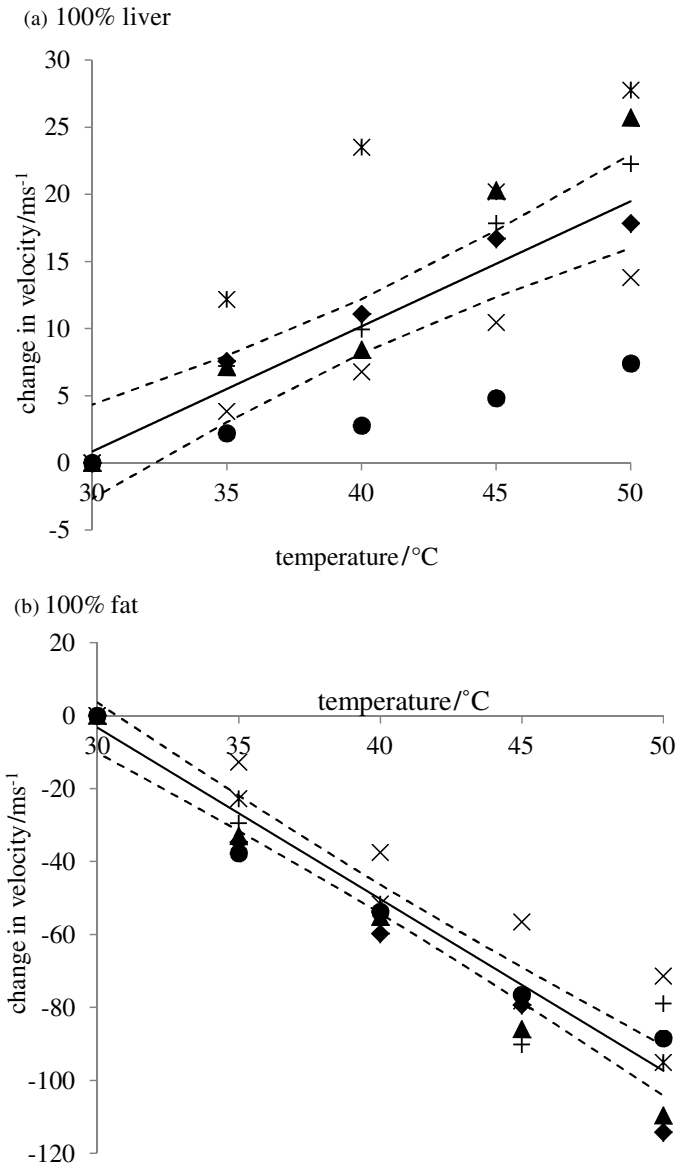

Figure 4. The change in propagation velocity of (a) 100% liver and (b) 100% fat with temperature. Individual samples of each tissue type are identified by symbols. For each data set the line of best fit is shown as a solid line and the 95% confidence interval for the slope of the line of best fit is shown as dashed lines.

ToF per °C) varies as a function of the percentage of fat in the sample (figure 5). Analysis showed that there was a linear increase in the temperature coefficient of the ToF with the percentage of fat in the sample ($r^2 = 0.89$) with the equation of the line of best fit having the form:

$$\frac{\Delta \mathrm{ToF}_{30}}{\Delta T_{30}} = af - b \tag{2}$$

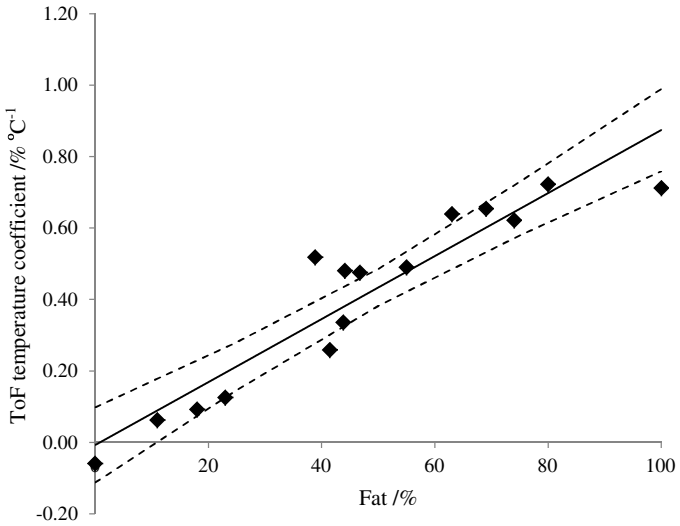

Figure 5. The change in ToF per °C with the percentage of fat in the sample. Individual measurements are shown together with the line of best fit (solid line) and the 95% confidence interval of the slope of the line of best fit (dashed lines).

where ΔToF_{30} is the percentage change in the ToF from the ToF at 30 °C, ΔT_{30} is the change in temperature from 30 °C, f is the percentage of fat in the sample and a and b are constants having values of 8.8×10^{-3} and 7.3×10^{-3} respectively.

3.2. Electrical impedance results

Figure 6(a) shows the electrical impedance spectra of the 100% liver samples as the temperature of the sample is raised from 30 to 50 °C in 5 °C steps. From figure 6(a) it can be seen that there is a single dispersion in the electrical impedance spectra of liver within the frequency range measured with the roll-off starting at about 8 kHz. The results presented in figure 6(b) show the electrical impedance measurements of the 100% fat samples as the temperature of the sample is raised from 30 to 50 °C in 5 °C steps. The results show that the electrical impedance of the fat is largely independent of frequency up to and including a frequency of 512 kHz, but there is a decrease in impedance at 1 MHz, the highest frequency measured.

Analysis of the change in impedance with temperature using the mean values plotted in figure 6 showed a linear decrease in impedance with increasing temperature for both liver and fat at all frequencies, but that the coefficient was different for different frequencies (figure 7). For fat there was little change in the temperature coefficient with frequency up to and including 256 kHz with no statistically significant correlation found between the temperature coefficient and the logarithm of frequency ($r^2 = 0.001$, $p = 0.92$). However, there was a positive linear correlation between the temperature coefficient and the logarithm of frequency for liver tissue ($r^2 = 0.92$, $p < 0.01$) with the slope of the line of best fit being 0.09% °C^{-1} log(kHz)$^{-1}$.

3.3. Combining ultrasound propagation velocity and electrical impedance measurements

The lack of a simple (linear) relationship between frequency and the temperature sensitivity of the electrical impedance for fat (figure 7), coupled with the large difference in the electrical impedance spectra between liver and fat (figure 6) and the need to normalize these spectra to remove the effect of the electrode geometry, suggested an approach of using the electrical

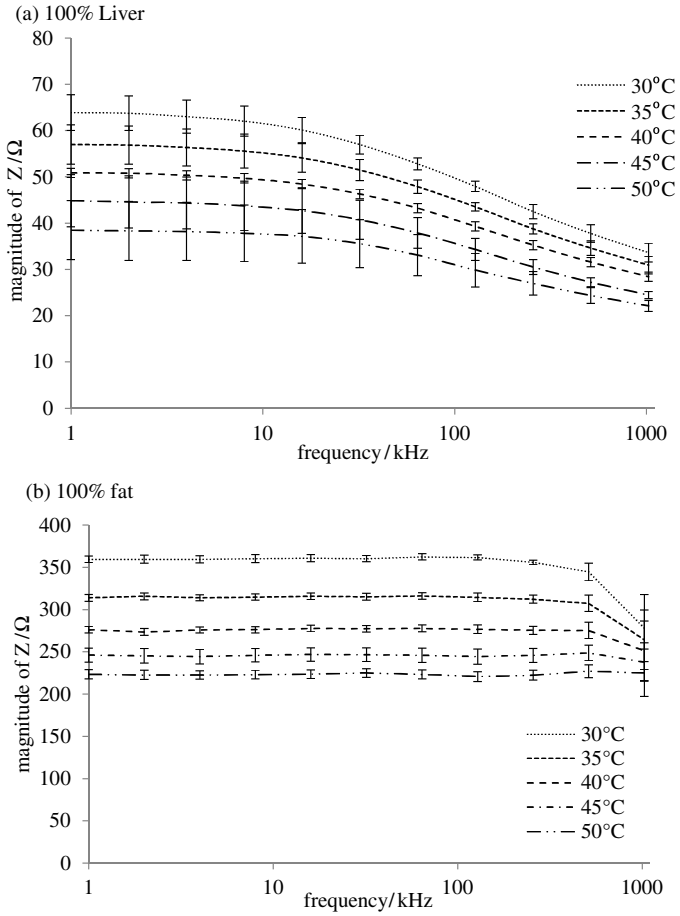

Figure 6. The effect of temperature on the electrical impedance spectra of (a) 100% liver and (b) 100% fat. The error bars on both graphs are ± 1 SEM.

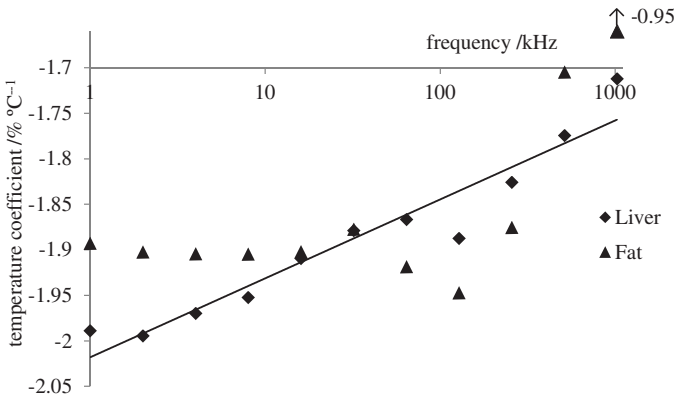

Figure 7. The tempereature sensitivity of the electrical impedance measurements shown in figure 6. The solid line is the line of best fit for the liver data. The coefficient at 1024 kHz for fat was much smaller (−0.95) than other values for both liver and fat and therefore has not been plotted to scale.

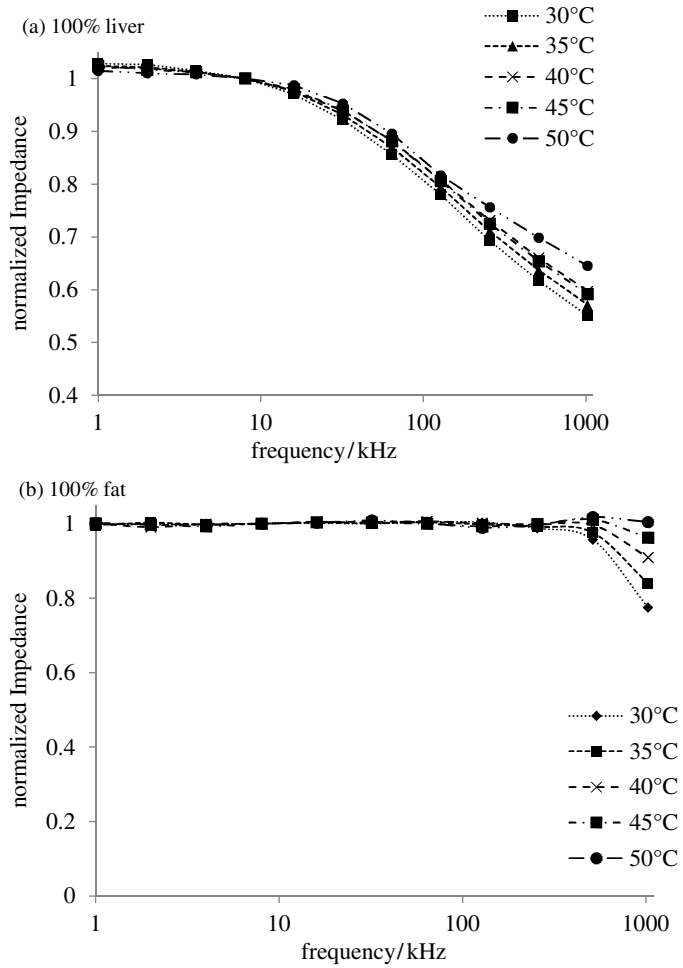

Figure 8. The electrical impedance spectra for (a) 100% liver and (b) 100% fat normalized to 8 kHz.

impedance to determine the fraction of fat in the sample and the ultrasound propagation velocity to determine the temperature using the relationship shown in figure 5.

If the impedance spectra were to be used to determine the percentage fat, then the normalized impedance spectra should have minimum temperature sensitivity. The error bars in figure 6(b) show the standard error in the impedance measurements for the 100% fat measurements. This plot shows that up to and including 256 kHz the variability of these measurements is small, rising from 1% at 30 °C to 3% at 50 °C. Above 256 kHz the variability is much larger having a maximum value of 13% for 1024 kHz at 30 °C. From figure 6(a) it can be seen that the variability in the measured impedance decreases with increasing frequency at all temperatures for the 100% liver measurements. Since the variability of the measurements decreases with increasing frequency, the frequency used to normalize the measurements, which also minimized the temperature variability, was taken as the highest measured frequency below the frequency of dispersion for the liver tissue. Therefore spectra from both 100% liver and 100% fat samples were normalized to the impedance at 8 kHz for each temperature, giving the normalized spectra for liver and fat shown in figures 8(a) and (b) respectively. The

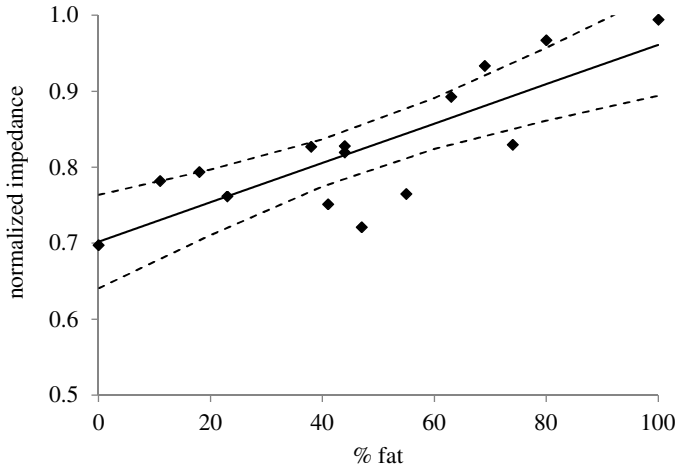

Figure 9. The change in the normalized impedance at 256 kHz with the percentage of fat in the sample. The solid line gives the line of best fit and the dashed lines the 95% confidence interval for its slope.

normalization of the impedance spectra to the impedance at 8 kHz reduced the temperature sensitivity of the measurements for liver to 0.20 $\pm$ 0.28% $^{\circ}C^{-1}$. From figure 8(a) it is clear that the normalized impedance at 50 $^{\circ}C$ is higher than those for the other temperatures at 256 kHz and above. If the temperature sensitivity is recalculated without the data at 50 $^{\circ}C$ the sensitivity for liver reduces to 0.001 $\pm$ 0.20% $^{\circ}C^{-1}$. For fat the temperature sensitivity of the normalized impedance data is 0.002 $\pm$ 0.035% $^{\circ}C^{-1}$ for frequencies up to and including 256 kHz.

Having minimized the temperature sensitivity of the electrical impedance measurements the next step was to determine the frequency at which the normalized impedance gave the best estimate of the percentage of fat in the sample. The candidate frequencies are those above the roll-off frequency in the spectrum for liver (8 kHz). In this study we have shown that there is a temperature sensitivity of the normalized electrical impedance of fat at 512 kHz and at 1 MHz. Therefore the frequency selected should be one of those measured between 8 and 256 kHz. The correlation between the percentage of fat by volume and the normalized impedance at 64, 128 and 256 kHz was determined from the electrical impedance spectra of the 15 layered samples measured in the same way as the fat and liver samples and then normalized to 8 kHz. The correlation analysis gave values of r^2 of 0.47, 0.54 and 0.65 at 64 kHz, 128 kHz and 256 kHz respectively. Whilst these values of r^2 are low, all were statistically significant at $p < 0.005$. Since the normalized impedance at 256 kHz gave the highest value of r^2, the normalized impedance at 256 kHz was selected to determine the percentage of fat in tissue samples (figure 9). The equation of the line of best fit for the data shown in figure 9 is given by:

$$Z_n = 2.6 \times 10^{-3} f + 0.70 \tag{3}$$

where Z_n is the impedance at 256 kHz normalized to the impedance at 8 kHz and f is the percentage of fat in the sample. Based on the t-statistic used to determine the 95% confidence interval of the line of best fit (Liengme 2002) and ten measurements, the predicted error in determining the fat content for the line of best fit at 5% fat is $\pm$26% and at 50% fat is $\pm$18%.

To evaluate the ability of the proposed technique to predict the temperature, a 15 cycle bootstrap analysis was run on the 15 layered tissue samples. For each cycle a single sample

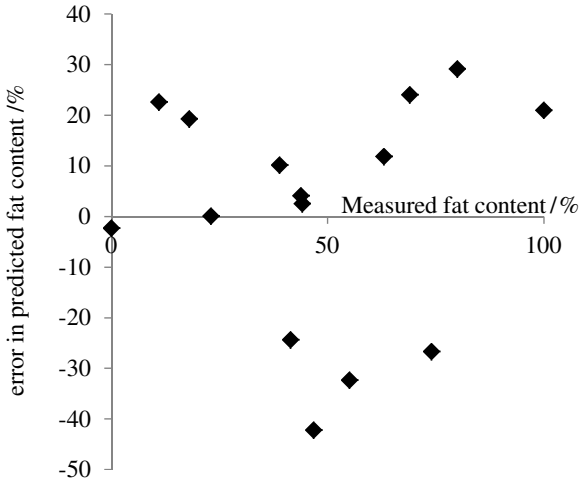

Figure 10. Error in estimating the fat content of the sample as a function of the measured fat content.

Table 1. The results from the bootstrap analysis where the temperature was predicted using the measured temperature coefficient of the ToF at 40 °C firstly using the normalized impedance at 256 kHz measured at 30 °C to predict the fat content and secondly using the measured fat content of the sample.

Sample number	Measured fat content (%)	Predicted fat content (%)	Measured temperature (°C)	Predicted temperature using predicted fat content (°C)	Predicted temperature using measured fat content (°C)
1	0	−2	40	117.2	−16.8
2	11	34	40	0.7	35.8
3	18	37	40	0.8	35.0
4	23	23	40	36.6	36.6
5	39	49	40	42.3	45.8
6	41	17	40	43.6	35.7
7	44	48	40	40.4	41.4
8	44	47	40	42.4	43.1
9	47	5	40	191.6	41.3
10	55	23	40	55.6	40.3
11	63	75	40	40.1	42.0
12	69	93	40	39.2	42.5
13	74	47	40	48.1	42.3
14	80	109	40	38.4	41.5
15	100	121	40	36.7	38.1

was omitted from the data set and the two lines of best fit re-calculated for the remaining 14 samples: the first between the temperature coefficient of the ToF and the percentage fat; and the second between the normalized impedance at 256 kHz and the percentage fat. The values obtained were then used to predict the temperature from the change in ToF for the omitted sample at 40 °C using: (a) the predicted fat composition from the normalized impedance at 30 °C; and (b) the measured fat content. The results from this analysis are shown in table 1.

Table 1 shows a large variation in the difference between the measured fat content and that predicted from the normalized impedance but there is no simple relationship between that difference and the percentage of fat in the sample (figure 10). For both the measured and the

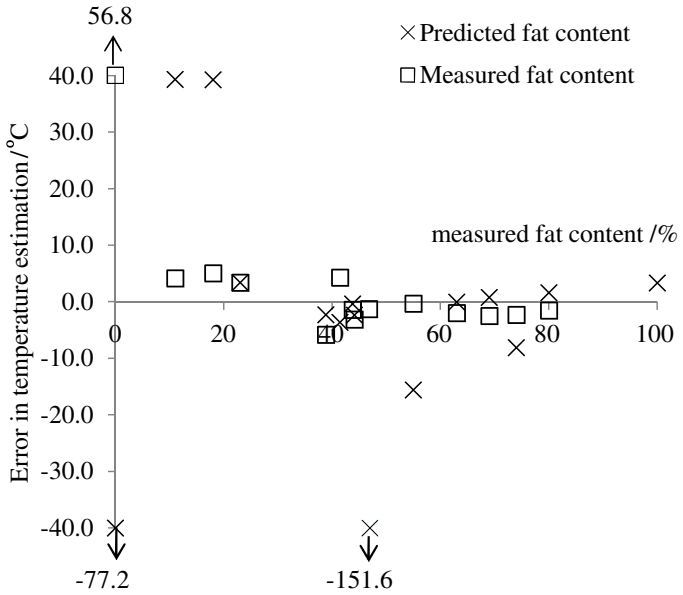

Figure 11. Error in estimating the temperature as a function of the measured fat content. Samples lying outside the range $\pm 50^{\circ}$ are not plotted to scale.

predicted fat content, the error in the temperature predicted from the ultrasound propagation velocity decreased with increasing fat content with that decrease being particularly noticeable for samples with more than 50% fat content (figure 11). From figure 5 it can be seen that the temperature coefficient for the ToF is close to zero for samples with a fat content close to zero and the effect of this can be seen in samples 1 and 9 in table 1. In both samples where either the predicted or measured fat content (or both) is close to zero there were large errors in the predicted temperature.

4. Discussion

The measured values for the changes in ultrasound propagation velocity with temperature for the 100% liver and 100% fat samples are in agreement with values obtained by others (Duck 1990). The results show a much greater inter-sample variability for liver than fat. Equation (1) predicts the propagation velocity of a sample of liver in terms of the volumetric fraction of condensed matter and fluids it contains. Whilst the origin of the inter-sample differences in propagation velocity for the liver is unclear, it is likely that a significant component of this could be due to differences in the fraction of condensed matter and fluid between samples. Differences in composition may also explain the sample with a much lower propagation velocity shown in figure 3. As noted by Miller *et al* (2004), separating the fluid and condensed matter to estimate the fraction of each would be difficult. Within this study we did attempt to do that by macerating liver tissue and then centrifuging it at 4500 rpm for 10 min but this failed to produce any separation. Optical microscopy of the centrifuged tissue confirmed the cellular structure was still intact. The only alternative is a chemical separation but the propagation velocity and masses of all the reactants and products, including gases, would need to be measured for inclusion in an analysis using equation (1).

The ultrasound propagation velocity for liver rises with increasing temperature to about 50 °C (Bamber 1998) and falls thereafter. This study shows that for the small temperature range between 30 and 50 °C the change can be approximated to be linear, however any nonlinearity will affect the confidence interval with which temperature can be predicted from a propagation velocity measurement. From the measurements made in this work the confidence intervals for predicting the temperature from a change in the propagation velocity for liver and fat were ± 4.3 °C and ± 1.7 °C at 40 °C respectively. To put this finding into context, measurements made on water and sunflower oil combined in a 80%/20% mixture using equation (1) gave a peak in the propagation velocity at 50 °C and a prediction error of ± 1.7 °C. The difference between this result and the measured results for fat and liver are due to variations in the tissue samples. It should be noted that a prediction error of ± 1.7 °C is above the 1 °C accuracy required clinically to deliver hyperthermia.

The amplitude of the reflected signal decreased with increasing temperature which has the effect of producing an increasing error in the propagation velocity determination as the temperature increased. This temperature dependence of the intensity of the reflected signal has previously been proposed as a possible method of non-invasively measuring the temperature where the property measured is termed the backscattered energy (Staube and Arthur 1994, Arthur *et al* 2003). The origin of this temperature dependence is multi-factorial but includes the temperature dependence of both the acoustic impedance and the attenuation of the propagating media (Staube and Arthur 1994). This temperature dependence combined with multiple reflections from interfaces in the layered tissue samples made the start of the reflected signal from the base of the test cell hard to reliably detect, limiting the accuracy with which the propagation velocity could be determined. Therefore the ToF based on the first large peak in the reflected signal has been used for the layered tissue experiments.

The analysis of the ultrasound ToF in the layered tissues showed a linear correlation between the percentage of fat in the sample and the change in the ToF. This finding is in agreement with the findings of Shannon *et al* (2004) who showed a linear correlation between propagation velocity and the lipid content of salmon muscle. These findings are also consistent with the relationship given in equation (1)—a relationship that was confirmed within this work through measurements on mixtures of sunflower oil and saline and sunflower oil and a lubricating oil (Mobil 10 W-40 semi-synthetic motor oil) in the test cell. Shannon *et al* (2004), as part of their work, derived a reciprocal squared relationship to relate the fraction of different components of a material and their individual propagation velocities to the overall propagation velocity of the material. However, there was a mathematical error in the derivation and, interestingly, they fitted a linear line to their measured data.

The original stimulus for the work reported in this paper was to explore the potential of using simultaneous ultrasound and electrical impedance measurements for surface determination of deep body temperature during mild hyperthermia used as part of cancer treatment. Whilst a linear relationship was found between the temperature coefficient of the ToF and the fat content (figure 5), the value of that coefficient is close to zero for small levels of fat in the tissue. Rearranging equation (2) and differentiating with respect to f gives the sensitivity of the change in temperature from 30 °C, $\Delta\mathrm{ToF}_{30}$, to the percentage fat content, f, in terms of the measured percentage change in the ToF from that at 30 °C:

$$\frac{\partial \Delta T_{30}}{\partial f} \approx \frac{-\Delta \mathrm{ToF}_{30}}{a(f-1)^2} \approx \frac{-100 \times \Delta \mathrm{ToF}_{30}}{(f-1)^2} \tag{4}$$

assuming $a \approx b \approx 10^{-2}$. Thus the sensitivity of the predicted temperature to errors in estimating the percentage of fat in the sample is a maximum at very low fat concentrations and decreases as the percentage of fat in the sample increases. The results from the bootstrap analysis confirm this as errors in the temperature predictions are large for a small fat content (figure 10) and

become smaller with increasing fat in the sample. Increasing the fat content of the sample has two effects: firstly, it increases the magnitude of the temperature sensitivity of the propagation velocity; and secondly, it reduces the effect of the nonlinearity in the propagation velocity characteristics of the water. Whilst normal tissue would typically have a substantial fat content, tumours only have a low fat content and therefore the approach proposed is unlikely to work in a simple manner for mild hyperthermia.

One possible solution to the low temperature coefficient of liver is to inject a non-ionic agent with a known linear propagation velocity temperature coefficient and thermal properties which is taken up equally by the tumour and the surrounding tissue. If the volume taken up could be determined by a cross-sectional imaging technique then equation (1) could be used to determine the effective propagation velocity of the agent and the liver. However, such an approach moves away from the original concept of a non-invasive measurement. As an initial exploration of the idea we measured the propagation velocity of a non-ionic x-ray contrast agent (Coviden Optiray 300 mg I ml^{-1}). The results of this together with the ToF results for liver combined using equation (1) suggested that adding 10% by volume of the contrast agent to liver would give a temperature coefficient for the ToF that would produce a good estimate of temperature based on the results obtained from the bootstrap analysis given in figure 11.

The well understood electrical impedance properties of tissue coupled with the lack of an intra-cellular fluid in fat cells makes electrical impedance measurement a candidate for the determination of the amount of fat in a sample. The results obtained for the 100% liver samples shown in figure 4(a) are consistent with a Cole–Cole model of cellular tissue (Cole and Cole 1941) although it should be noted that the highest frequency measured, 1 MHz, was below the frequency at which the impedance plateaus. The minimal change in impedance of the 100% fat samples with frequency up to 512 kHz is consistent with fat cells having no intra-cellular fluid. However, the lipid within fat cells is a dielectric and the decrease in impedance at 1 MHz is consistent with this and has been confirmed by modelling (Islam 2012).

The results for the 100% liver samples show a decrease in the variability of the measured electrical impedance with frequency. Whilst the origins of this are unclear, the findings may be due to the differences in the volume of extra-cellular fluid between samples. It should be noted that this is analogous to the potential explanation for the variability found in the results on the ultrasound propagation velocity in liver. In contrast, the variability in the electrical impedance measurements for the 100% fat samples was much smaller and independent of frequency. On epithelial tissues, differences in cellular structure have been shown to produce differences in the parameters of Cole–Cole models fitted to measured electrical impedance spectra (Brown *et al* 2000b, Gonzalez-Correa *et al* 1999). Within the context of this study, differences in dispersion frequency or fitted parameters might have provided information on the fluid and condensed matter content of the liver, but neither the frequency range nor the frequency resolution allowed this to be investigated.

The electrode geometry, and in particular, the electrode spacing, determines the absolute value of the measured impedance and therefore the spectra must be normalized to allow comparisons between studies. Within this study, normalization was also required to minimize the temperature sensitivity of the spectra. In choosing a low frequency to normalize the impedance measurements both the inter-sample variability and the effect of temperature must be taken into consideration as the former will have the effect of increasing the variability of the normalized high frequency values. Results obtained in this study show there is little temperature sensitivity below 256 kHz for fat and a linearly decreasing negative sensitivity with frequency for liver. The change in the temperature coefficient with frequency for the liver samples will also result in increased temperature sensitivity of the high to low frequency

ratio as the difference between the two frequencies increases. Therefore 8 kHz, the highest frequency below the roll-off in impedance for the liver tissue, was selected.

A good correlation and a line of best fit with a small confidence interval for the slope is required between the normalized impedance and the percentage of fat in the sample if the normalized impedance is to be used to determine the percentage of fat in the tissue. All the frequencies examined gave a statistically significant correlation coefficient ($p < 0.005$) with the percentage of fat but the use of 256 kHz gave the largest value of r^2 (0.65). However this is still small and gave a consequently large confidence interval for any predictions. This result is poorer than might have been expected given the results for fat and liver when measured separately. This may be due to one of the underlying problems of tetrapolar impedance measurement: that of a complex sensitivity distribution coupled with regions of negative sensitivity between the drive and receive electrodes (Islam *et al* 2010, Brown *et al* 2000a). We have previously shown (Islam *et al* 2010) that the sensitivity distribution can be improved through summing multiple measurements made using different combinations of electrodes over the region of interest (Rabbani and Karal 2008). However, even with this approach a complex sensitivity distribution results with regions of negative sensitivity close to the electrodes (Islam *et al* 2010). Further improvement in the spatial distribution of sensitivity for tetrapolar impedance measurements is required before the technique proposed in this paper can be considered as a potential measurement technique in clinical mild hyperthermia.

The work reported in this paper has not used living tissue and the values for the temperature coefficient of the impedance obtained for fat and liver are consistent with that of physiological saline ($-2\%\ ^{\circ}C^{-1}$, Duck 1990). Gersing *et al* (1995) reported that different living tissues yielded different temperature coefficients for electrical conductivity. It is unclear whether these differences are the result of the non-electrolyte components of the tissue or metabolic changes associated with heating (e.g. changes in blood flow and membrane conductivity). In a later study Gersing (1999) reported that the onset of changes in the electrical impedance of malignant tissue was delayed when compared with normal tissue.

The results reported in this study have quantified the changes in electrical impedance spectra and propagation velocity for liver and fat and have measured both in a layered tissue model to establish the effect of fat on both temperature coefficients. Whilst linear relationships were found, the confidence intervals from the predictions of fat and temperature, particularly the latter, were not adequate for the combination of measurements to provide a tool for use in the clinical environment. The variability in the measurements has been quantified and possible sources identified. Further work is required to determine whether these can be minimized to the level where a clinically useful tool can be implemented.

Acknowledgments

NI gratefully acknowledges support from the British Council for a Commonwealth Scholarship award. The authors also knowledge support from T F Yu, who was funded through the Wellcome Trust Vacation Scholarship scheme to implement the prototype of the electrical impedance measurement instrumentation.

References

Aitkenhead A H, Mills J A and Wilson A J 2008 The design and characterization of an ultrasound phased array suitable for deep tissue hyperthermia *Ultrasound Med. Biol.* **34** 1793–807

Aitkenhead A H, Mills J A and Wilson A J 2009 An analysis of the origin of differences between measured and simulated fields produced by a 15 element ultrasound phased array *Ultrasound Med. Biol.* **36** 410–8

Apfel R E 1983 The effective nonlinearity parameter for immiscible liquid mixtures *J. Acoust. Soc. Am.* **74** 1866–8
Arthur R M, Straube W L, Starman J D and Moros E G 2003 Noninvasive temperature estimation based on the energy of backscattered ultrasound *Med. Phys.* **30** 1021–9
Bamber J C 1998 Acoustical characteristics of biological media *Encyclopedia of Acoustics* vol 4 ed M J Crocker (New York: Wiley) pp 1703–26
Brown B H, Tidy J A, Boston K, Blackett A D, Smallwood R H and Sharp F 2000b Relation between tissue structure and imposed electrical current flow in cervical neoplasia *Lancet* **355** 892–5
Brown B H, Wilson A J and Bertemes-Filho P 2000a Bipolar and tetrapolar transfer impedance measurements from a volume conductor *Electron. Lett.* **36** 2060–2
Chambre P L 1959 Speed of a plane wave in a gross mixture *J. Acoust. Soc. Am.* **26** 329–31
Cole K S and Cole R H 1941 Dispersion and absorption in dielectrics *J. Chem. Phys.* **9** 341–51
Conway J, Hawley M S, Seagar A D, Brown B H and Barber D C 1985 Applied potential tomography (APT) for noninvasive thermal imaging during hyperthermia treatment *Electron. Lett.* **21** 836–8
Del Grosso V A and Madder C W 1972 Speed of sound in pure water *J. Acoust. Soc. Am.* **52** 1442–6
Duck F 1990 *Physical Properties of Tissue* (London: Academic)
Esrick M A and McRae D A 1994 The effects of hyperthermia-induced tissue conductivity changes on electrical impedance temperature mapping *Phys. Med. Biol.* **39** 133–44
Ferraioli F, Formisano A and Martone R 2009 Effective exploitation of prior information in electrical impedance tomography for thermal monitoring of hyperthermia treatments *IEEE Trans. Magn.* **45** 1554–7
Gersing E 1999 Monitoring temperature-induced changes in tissue during hyperthermia by impedance methods *Ann. New York Acad. Sci.* **873** 13–20
Gersing E, Krüger W, Osypka M and Vaupel P 1995 Problems involved in temperature measurements using EIT *Physiol. Meas.* **16** A153–60
Gonzalez-Correa C A, Brown B H, Smallwood R H, Kalia N, Stoddard C J, Stephenson T J, Haggie S J, Slater D N and Bardhan K D 1999 Virtual biopsies in Barrett's esophagus using an impedance probe *Ann. New York Acad. Sci.* **873** 313–21
Islam N 2012 The potential for using combined electrical impedance and ultrasound measurements for the non-invasive determination of temperature in deep body tumours during mild hyperthermia *PhD Thesis* University of Warwick
Islam N, Rabbani K S-E and Wilson A 2010 The sensitivity of focused electrical impedance measurements *Physiol. Meas.* **31** S97–S109
Kell G S 1975 Density thermal expansivity and compressibility of liquid water from 0–150 °C correlations and tables for atmospheric pressure and saturation reviewed and expressed on 1968 temperature scale *J. Chem. Eng. Data* **20** 97–105
Lagendijk J J W 2000 Hyperthermia treatment planning *Phys. Med. Biol.* **45** R61–R76
Liengme B V 2002 *Guide to Microsoft Excel for Scientists and Engineers* (Oxford, UK: Butterworth-Heinemann)
Miller N R, Bamber J C and Meaney P M 2002 Fundamental limitations of non-invasive temperature imaging by means of ultrasound echo strain estimation *Ultrasound Med. Biol.* **28** 1319–33
Miller N R, Bamber J C and ter Haar G R 2004 Imaging of temperature-induced echo strain: preliminary *in vitro* study to assess feasibility for guiding focused ultrasound surgery *Ultrasound Med. Biol.* **30** 345–56
Moskowitz M J, Paulsen K D, Ryan T P and Pang D 1994 Temperature field estimation using electrical impedance profiling methods: II. Experimental system description and phantom results *Int. J. Hyperthermia* **10** 229–45
Paulson K D and Jiang H 1997 An enhanced electrical impedance imaging algorithm for hyperthermia applications *Int. J. Hyperthermia* **13** 459–80
Persson H W and Hertz C H 1985 Acoustic impedance matching of medical ultrasound transducers *Ultrasonics* **23** 83–89
Rabbani K S and Karal M A S 2008 A new four electrode focused impedance measurement (FIM) system for physiological study *Ann. Biomed. Eng.* **36** 1072–7
Rieke V and Pauly K B 2008 MR thermometry *J. Magn. Reson. Imaging* **27** 376–90
Sauer R, Creeze H, Hulshof M, Issels R and Ott O 2012 Concerning the final report 'Hyperthermia: a systematic review' of the Ludwig Boltzmann Institute for Health Technology Assessment, Vienna, March 2010 *Strahlenther. Uud Onkol.* **188** 209–13
Seip R and Ebbini E S 1995 Noninvasive estimation of tissue temperature response to heating fields using diagnostic ultrasound *IEEE Trans. Biomed. Eng.* **42** 828–39
Shannon R A, Probert-Smith P J, Lines J and Mayia F 2004 Ultrasound velocity measurement to determine the lipid content in salmon muscle; the effects of myosepta *Food Res. Int.* **37** 611–20
Staube W L and Arthur R M 1994 Theoretical estimation of the temperature dependence of backscattered ultrasonic power for noninvasive thermometry *Ultrasound Med. Biol.* **20** 915–22

ter Haar G R 1999 Therapeutic ultrasound *Eur. J. Ultrasound* **9** 3–9

Triantopoulou S, Efstathopoulos E, Platon K, Uzunoglou N, Kelekis N and Kouloulias V 2013 Radiotherapy in conjunction with superficial and intracavitary hyperthermia for the treatment of solid tumours: survival and thermal parameters *Clin. Transl. Oncol.* **15** 95–105

van Rhoon G C and Wust P 2005 Non-invasive thermometry for thermotherapy *Int. J. Hyperthermia* **21** 489–95

Wilson A J, Milnes P, Waterworth A R, Smallwood R H and Brown B H 2001 Mk3.5: a modular, multi-frequency successor to the Mk3a EIT/EIS *Syst. Physiol. Meas.* **22** 49–54